LXR and ABCA1 control cholesterol homeostasis in the proximal mouse epididymis in a cell-specific manner

Aurélia Ouvrier,* Rémi Cadet,* Patrick Vernet,* Brigitte Laillet,[†] Jean-Michel Chardigny,[†] Jean-Marc A. Lobaccaro,* Joël R. Drevet,[1],* and Fabrice Saez*

Université Blaise Pascal,* Unité Mixte de Recherche GReD Centre National de la Recherche Scientifique 6247, INSERM U931, 63177 Aubiere, cedex, France; and Unité Mixte de Recherche 1019,[†] Institut National de la Recherche Agronomique/Université d'Auvergne Laboratoire de Nutrition Humaine, Clermont-Ferrand, cedex 1, France

Abstract Mammalian spermatozoa undergo important plasma membrane maturation steps during epididymal transit. Among these, changes in lipids and cholesterol are of particular interest as they are necessary for fertilization. However, molecular mechanisms regulating these transformations inside the epididymis are still poorly understood. Liver X receptors (LXRs), the nuclear receptors for oxysterols, are of major importance in intracellular cholesterol homeostasis, and LXR$^{-/-}$-deficient male mice have already been shown to have reduced fertility at an age of 5 months and complete sterility for 9-month-old animals. This sterility phenotype is associated with testes and caput epididymides epithelial defects. The research presented here was aimed at investigating how LXRs act in the male caput epididymidis by analyzing key actors in cholesterol homeostasis. **We** show that accumulation of cholesteryl esters in LXR$^{-/-}$ male mice is associated with a specific loss of ABCA1 and an increase in apoptosis of apical cells of the proximal caput epididymidis. ATP-binding cassette G1 (ABCG1) and scavenger receptor B1 (SR-B1), two other cholesterol transporters, show little if any modifications. Our study also revealed that SR-B1 appears to have a peculiar expression pattern along the epididymal duct. These results should help in understanding the functional roles of LXR in cholesterol trafficking processes in caput epididymidis.—Ouvrier, A., R. Cadet, P. Vernet, B. Laillet, J-M. Chardigny, J-M. A. Lobaccaro, J. R. Drevet, and F. Saez. **LXR and ABCA1 control cholesterol homeostasis in the proximal mouse epididymis in a cell-specific manner.** *J. Lipid Res.* 2009. 50: 1766–1775.

Supplementary key words apical cells • ATP-binding cassette G1 • scavenger receptor B1 • liver X receptors • ATP binding cassette transporter

The epididymis is an essential organ for reproductive physiology as sperm cells start the process of posttesticular maturation during their transit in this organ. This migration will transform the immotile and unfecondant spermatozoa to fully mature cells (1, 2). Principal aspects of epididymal transformation include functional maturation, sperm concentration, storage of the spermatozoa in a quiescent state, and removal of degenerating cells. Functional maturation of these spermatozoa requires interaction of sperm with luminal fluid, whose composition is regulated by absorption and secretion activities of the epididymal epithelium (3).

The sperm plasma membrane is the site of dramatic changes throughout the development of these cells, and, in the epididymis, the remodeling process includes important modifications in lipid composition as well as repositioning of lipid and protein components to different membrane domains (4). The lipid composition of mammalian spermatozoa is specific with a large amount of plasmalogen phospholipids (PLs), a high content of long-chain PUFAs, mostly arachidonic acid (20:4, n-6), docosapentaenoic acid (22:5, n-3), and docosahexaenoic acid (22:6, n-3), and relatively low cholesterol:PL ratios ranging from 0.24 for caput epididymidis sperm to 0.29 for cauda epididymidis sperm in mice (5). This ratio is an indicator of membrane fluidity, and although it is quite stable during epididymal transit, membrane fluidity was shown to increase during this step (6). Earlier work showed a significant decrease of the two major PLs, phosphatidylcholine and phosphatidylethanolamine, in mouse spermatozoa from cauda epididymidis compared with those from caput epididymidis (5). During epididymal maturation, stearic acid (C18:0) decreased also, whereas palmitic acid (C16:0) increased. Among the PUFAs, docosapentaenoic and docosahexaenoic acids rose significantly in the cauda epididymidis. Cholesterol content also declined by roughly 65% during epididymal maturation (5). These modifications have been supposed to prepare sperm cells for capacitation and acrosome reaction that take place in the

[1]To whom correspondence should be addressed.
e-mail: joel.drevet@univ-bpclermont.fr

This article is available online at http://www.jlr.org

female genital tract and that are fundamental for fertilization to occur (7, 8). During capacitation, cholesterol depletion appears to be critical for the activation of tyrosine kinases leading to changes in protein conformation of the sperm membrane and cholesterol efflux leading to Ca^{2+} influx, which in turns allows the development of motility (9). Membrane cholesterol is thus a key player in the acquisition of spermatozoa fertilizing potential; paradoxically, molecular events regulating this process are still poorly understood.

Among the various transcription factors that regulate cholesterol homeostasis, liver X receptors (LXRs) have specific roles. While LXRα (NR1H3) is expressed in tissues that have an important lipid metabolism, such as testis and liver, LXRβ (NR1H2) has a rather ubiquitous expression. They are both activated by oxysterols (10). LXRs have been associated with various physiological functions (for a review, see Ref. 11), such as reverse cholesterol transport by the induction of the ATP-binding cassette proteins ABCA1 and ABCG1. The importance of LXR in the male reproductive physiology was underlined by the $LXR^{-/-}$ mice model. These mice showed male infertility starting at around 5 months of age and progressively became sterile after 9 months (12). In the testis, the loss of germ cells, a decreased testicular testosterone level, and lipid accumulation were described (13, 14). In addition, considerable destructuration of the caput epididymidis epithelium was observed, characterized by a reduction of cell height specifically located in proximal segments 1 and 2. Moreover, loss of LXR was shown to result in perturbations of caput epididymidis lipid content with cholesteryl ester (CE) accumulations located in the epithelium as well as in peritubular tissue (15). In addition, spermatozoa from 9-month-old $LXR^{-/-}$ male mice and older showed a loss of their flagella in most of the cases, probably due to excessive fragility of their mid-piece (15).

This article further investigates the roles of LXR in caput epididymidis physiology. The data presented here show that LXRs play a central role in epididymal cholesterol homeostasis by regulating ABCA1 in a segment and cell-type-specific manner, providing new insights about molecular mechanisms regulating sperm cell maturation process and fertility.

MATERIALS AND METHODS

Animals and tissue preparation

Wild-type and $LXR^{-/-}$ male mice were euthanized by decapitation as previously described (13). These mice came from a hybrid line C57BL6 × 129 SVJ and were housed in an animal facility with controlled environment (temperature = 22°C, 12 h light/12 h dark). In normal conditions, these mice were fed ad libitum with Global-diet-2016S (cholesterol free) from Harlan (Gannat, France). For the Western diet, animals were fed during 7 weeks ad libitum with a 1.25% cholesterol-enriched diet (Safe, Augy, France). Housing and manipulation of these animals were approved by the Regional Ethic Committee in Animal Experimentation (authorization CE2-04).

Nile Red staining of lipids

Seven-micrometer-thick cryosections were mounted on Superfrost® plus glass slides (Menzel Glaser® Templemars, Paris, France). Cryosections were equilibrated for 5 min in PBS, fixed for 5 min in 4% paraformaldehyde-PBS, rinsed in PBS, and then incubated at 4°C in a humidified chamber with the Nile Red solution (2 µg/ml in PBS). Sections were counterstained with Hoechst 33342 solution (1 µg/ml; Sigma-Aldrich, St Quentin Fallavier, France) and mounted with coverslips using PBS-glycerol (v/v) as mounting medium. Nile Red is only fluorescent when incorporated in a hydrophobic environnement. For cells stained with Nile Red and excited with blue (wavelength: 488 nm), membranes fluoresce in deep red (wavelength: >650 nm) due to PLs. Endosomes containing neutral lipids, such as triglycerides, cholesterol, or CEs, fluoresced in green (wavelength: ≈530 nm).

Quantification of mRNA by real-time quantitative RT-PCR

Real-time quantitative PCR was performed with the Bio-Rad I-Cycler and the IQ^{TM} SYBR® Green Supermix Bio-Rad mix (Bio-Rad, Marne-la-coquette, France). Two microliters of 1:50 diluted cDNA template were amplified by 0.5 units of HotMaster TaqDNA polymerase (Bio-Rad) using SYBR Green dye to measure duplex DNA formation following the manufacturer's instructions. Primer sequences are given in **Table1**. Quantification was obtained from the relation between the threshold cycle value and a standard curve (16).

Immunohistochemistry

Seven-micrometer-thick paraffin sections were mounted on Superfrost® glass slides and then deparaffinized with Histoclear for 40 min (National Diagnostic, Merck Eurolab, Fontenay-sous-Bois, France), rehydrated through a graded series of ethanol solutions, and finally rinsed in distilled water.

Peroxydase detection. To inhibit endogen peroxidases, slides were placed 30 min in 0.3% H_2O_2 in water. Sections were then treated using the Vectastain® ABC Kit Rabbit peroxydase IgG (Vector Laboratories, Abcys, Paris, France) according to the manufacturer's instructions. The primary antibody, rabbit-polyclonal anti SR-B1 (1/2,000 in PBS-Normal Goat Serum 0.1%; Novus Biological, Interchim, Montluçon, France), was incubated overnight at 4°C in a humidified chamber. The revelation was obtained with the Vector NovaRED substrate kit for peroxydase (Vector Laboratories) for 10 min. Slides were counterstained with Hematoxylin QS (Vector Laboratories) for 20 s and mounted with coverslips using Cytoseal 60 mounting medium (Electron Microscopy Sciences, Hatfield, USA).

Immunofluorescence detection. After deparaffinization, sections were equilibrated 5 min in PBS and blocked in PBS containing 1% (w/v) BSA (Euromedex, Mundolsheim, France) and 1% (w/v) fetal calf serum for 30 min. The slides were then incubated overnight at 4°C in a humidified chamber with the primary antibody, which was either rabbit polyclonal anti-ABCG1 (1/500; Novus Biological) or rabbit polyclonal anti-ABCA1 (1/500; Novus Biological) diluted in PBS containing 0.1% (w/v) BSA. Sections were washed for 5 min in PBS, blocked for 20 min in 1% PBS-BSA and then incubated with FITC-conjugated secondary goat anti-rabbit Alexa 488 antibodies (1/1,000 in PBS-0.1% BSA; Invitrogen). Sections were counterstained with Hoechst 33342 solution (1 µg/ml; Sigma-Aldrich) and mounted with coverslips using PBS-glycerol (v/v).

In situ cell death detection

After deparaffinization as described above, sections were treated with the In Situ Cell Death Detection Kit (Roche

TABLE 1. Sequences of primers used for quantification of mRNA by real-time quantitative RT-PCR

	GenBank Accession Number	Primer Forward (5′→3′)	Primer Reverse (5′→3′)	Tm	Size
Abca1	NM_013454	GGAGCTGGGAAGTCAACAAC	ACATGCTCTCTTCCCGTCAG	56°C	176 bp
Abcg1	NM_009593	GCTGTGCGTTTTTGGCTGTT	TGCAGCTCCAATCAGTAGTCCTAA	63°C	84 bp
Acat1	NM_144784	ATTTGCTGATGCTGCCGTAG	TTTTGGGGGTCAATCTCCAG	64°C	177 bp
Acat2	NM_005891.2	CACCCCAGCGAACGCATC	GAGGGTATTGTCTTCCGAGG	59°C	147 bp
Cyclophillin	NM_008907.1	GGAGATGGCACAGGAGGAA	GCCCGTAGTGCTTCAGCTT	62°C	75 bp
hmgcoaR	NM_008255	CTTGTGGAATGCCTTGTGATT	AGCCGAAGCAGCACATGAT	64°C	75 bp
hmgcoaS	NM_145942	TGACATGCTCTCCGAGTACC	CAGGAACATCCGAGCTAGAG	64°C	220 bp
Srebp2	NM_033218	GTTGACGCAGACAGCCAATG	CCCTTACTGGCACTTGAAGG	64°C	241 bp

Diagnostics, Grenoble, France) according to the manufacturer's instructions. Briefly, the principle of this kit is the labeling of DNA strand breaks by terminal deoxynucleotidyl transferase, which catalyzes polymerization of labeled nucleotides to free 3′-OH DNA ends in a template-independent manner [terminal desoxynucleotidyl transferase-mediated dUTP nick end labeling (TUNEL) reaction].

Western blot analysis

Proteins (40 μg) were separated by SDS-PAGE and transferred onto nitrocellulose membrane (Hybond ECL; Amersham Biosciences, France). Blots were blocked with 10% low-fat dried milk/0.1% Tween 20/Tris base salt and then incubated with either anti-β actin (1/5,000; Sigma-Aldrich), anti-ABCA1 (1/500), anti-ABCG1 (1/1,000), or anti-SRB1 (1/2,000). Detection was performed with the goat anti-rabbit horseradish peroxidase-conjugated secondary antibodies (1/5,000; Amersham) using the ECL Western Blotting Detection kit (Amersham) on hyperfilms (Amersham). Densitometric analyses were carried out with Quantity One software (Bio-Rad).

Gas chromatography

Total lipids from caput epididymides were extracted using chloroform/methanol based on the Folch method and then diluted in 100 μl chloroform. Total lipids were separated into nonpolar lipids or neutral lipids and PLs by the using Sep-pak® column silica cartridges (Sep-Pak, vac 1 cc, 100 mg; Waters, Guyancourt, France) as described by Juaneda and Roquelin (17). Briefly, after washing the column with 4 ml of chloroform, the samples of total lipid extracts were loaded on the top of the cartridges. Nonpolar lipids were eluted with 4 ml of chloroform, following which the fraction containing the PLs was eluted with 8 ml of methanol. Lipids were then evaporated under a nitrogen flux and diluted in 100 μL of toluene and 200 μl methanol. Lipids were methylated for 20 min at 20°C with 100 μl of 2 N sodium methanolate (Sigma-Aldrich), followed by a 20 min incubation with 500 μl 14% BF3/methanol (Sigma-Aldrich). After washing with saturated NaHCO$_3$, methyl esters were extracted with 2 ml hexane, vortex and evaporation of the top hexanic phase. Before analysis, the neutral lipid fraction was loaded on a Florisil cartridge (Chromabond® 6 ml/500 mg; Macherey-Nagel, Hoerdt, France) preconditioned with hexane and then eluted with a mixture of hexane:ethylic ether (95:5, v:v). Methyl esters were concentrated, diluted in 200 μl hexane, and stored at −80°. Before analysis, samples were filtered on a florisil column, eluted with a mixture of hexane:ethylic ether (95:5, v:v), evaporated, and diluted in a known volume of hexane. The analysis was performed on a GC trace gas chromatograph (Thermo Electron, Courtaboeuf, France) equipped with a capillary DBWAX column (30 m, 0.25 mm, 0.25 μm thick; JW Scientific, Folsom, CA). The injector was a split-splitless type and the detector a flame ionization detection type. Fatty acid methyl esters

were characterized in quality and quantity by comparing their retention times to those obtained from a known mixture (MIX37 from Sigma-Aldrich).

Statistical analyses

A Student's *t*-test was performed to determine significant differences between groups with *P* value < 0.05.

RESULTS

Age-related CE accumulation in caput epididymidis of LXR$^{-/-}$ mice

Previous studies had shown that homozygous deletion of *lxr* resulted in CE accumulation in the epididymis of the LXR$^{-/-}$ animals (15). To determine which cells among the different cell types constituting the epididymal epithelium (**Fig. 1A**) are concerned by these accumulations, we used Nile Red staining on caput epididymidis sections of 4- and 9-month-old wild-type and LXR$^{-/-}$ mice. No neutral lipid accumulation was observed in caput epididymidis segments 1 and 2 from wild-type mice, whereas lipid droplets were visible in LXR$^{-/-}$ mice at 4 and 9 months of age (Fig. 1B) in the same segments. These accumulations were mainly localized in interstitial cells surrounding the tubules as well as in one subtype of epithelial cells: the so-called apical cells (Fig. 1C, arrows). These neutral lipid stainings in apical cells were limited to segments 1 and 2 of the caput epididymides (data not shown).

Cholesterol de novo synthesis does not seem to be responsible for CE accumulation

To check whether increased de novo cholesterol synthesis was responsible for CE increase, the expression of genes encoding cholesterol and CE producing enzymes was measured by quantitative RT-PCR. This included *acyl-CoA cholesteryl acyltransferase1* (*acat1*) and *acat2*, which esterify free cholesterol and store CE in lipid droplets; *sterol regulatory element binding factor 2* (*srebp2*), which regulates the de novo synthesis of cholesterol; and *3-hydroxy-3-methyl-glutaryl-coA-reductase* (*hmg-coA-red*) and *3-hydroxy-3-methyl-glutaryl-coA-synthase* (*hmg-coA-synt*), the rate-controlling enzymes of the mevalonate pathway that produces cholesterol and other isoprenoids. Expression levels of *acat1*, *acat2*, and *hmg-coA-red* were not significantly modified (**Fig. 2**), while *srebp2* and *hmg-coA-synt* expression was decreased by 42 ± 5% (*P* < 0.01) and 48 ± 6.5% (*P* < 0.01), respectively, in
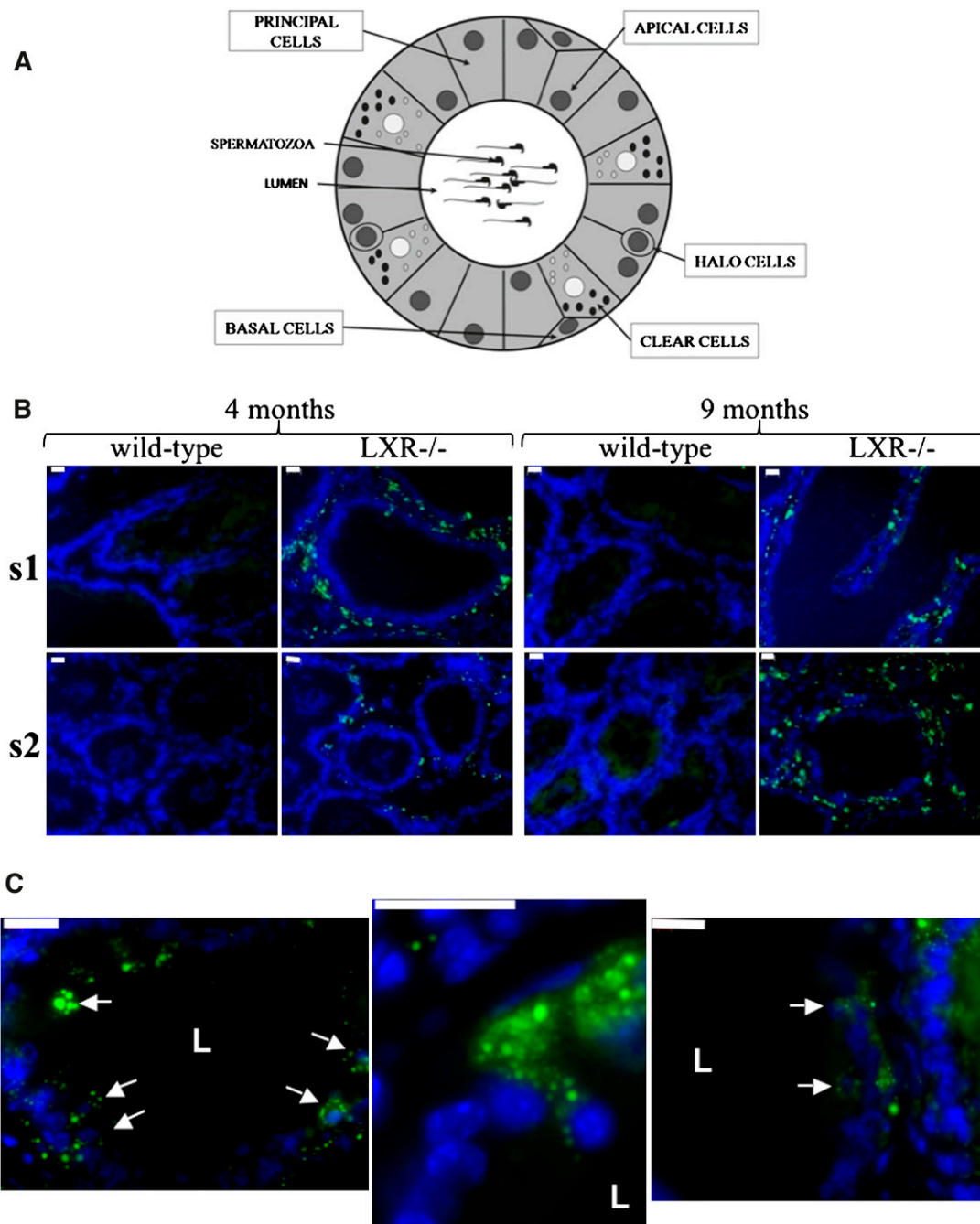
Fig. 1. Neutral lipid accumulation appeared in LXR$^{-/-}$ mice from 4 months of age. A: Schematic representation of organization of the epididymis epithelium. B: Nile Red staining on segment 1 (s1) and segment 2 (s2) caput epididymidis from wild-type and LXR$^{-/-}$ mice at 4 and 9 months of age. Green fluorescence indicates neutral lipid accumulations. Each micrograph is representative of three different experiments made on three different individuals. Bars = 20 µm. C: LXR$^{-/-}$ mice 4 and 9 months old at higher magnification. Bars = 20 µm. Arrows indicate lipid accumulation in apical cells as evidenced by their apical located nuclei (enlarged in the center panel). L indicates the position of the luminal compartment.

LXR$^{-/-}$ mice compared with the wild-type. Endogenous synthesis of cholesterol was thus not responsible for CE accumulation.

Cholesterol uptake does not seem to be responsible for CE accumulation

Cholesterol uptake was investigated by studying the presence of SR-B1 by immunohistochemistry. As shown in **Fig. 3A**, SR-B1 presented a segment-dependent localiza-tion pattern. In segment 1, SR-B1 was localized in the vascular endothelium (Fig. 3B, arrows) and in the apical and basal membranes of the epithelium (Fig. 3B). The same localization was observed in segment 2, but apical membrane staining systematically appeared stronger. In segment 3, staining was diffuse in the cytoplasm of epithe-lial cells, sometimes presenting stronger punctual staining that could have been due to the presence of SR-B1 on intracellular organelles, such as endosomes. No change
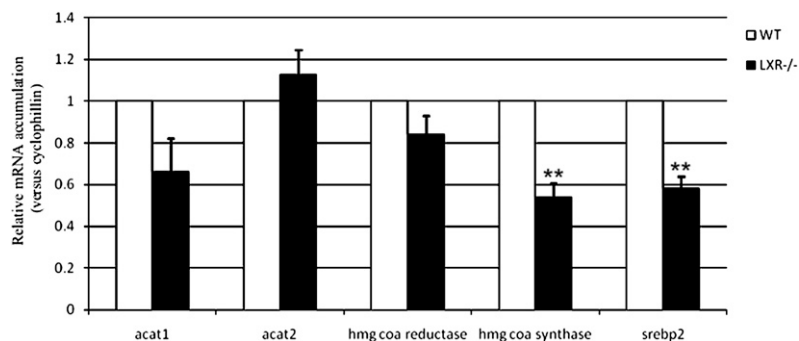
Fig. 2. Relative expression level of six genes involved in cellular cholesterol homeostasis in 8-month-old wild-type and LXR$^{-/-}$ mice. Relative expression level of *acat1, acat2, hmg coa red, hmg coa synt,* and *srebp2* mRNAs in caput epididymides measured by quantitative RT-PCR. Histograms are expressed as a normalized value of the expression level in lxr$^{-/-}$ animals versus an arbitrary value of 1 in the wild-type animals. Each value is the mean ± SEM of three measurements performed on three different animals using cyclophillin as internal standard. **$P < 0.01$ compared with wild-type mice.

was observed at 9 months of age. The LXR$^{-/-}$ mice presented the same pattern in segment 3. The main difference was observed in segments 1 and 2 where both staining and epithelium height decreased significantly. This reduced signal was not correlated with Western blot analysis of SR-B1 (Fig. 3C). These results suggested that SR-B1 was not directly responsible for the neutral lipid accumulation observed. In addition, LDL receptor (LDLR) localization was studied, and no difference observed (data not shown).

Loss of ABCA1 is related to CE accumulation

Since de novo cholesterol synthesis and cholesterol uptake did not seem to be at stake to explain CE accumulation in the caput epididymidis of LXR$^{-/-}$ mice, we analyzed the localization and distribution of two membrane cholesterol transporters involved in cholesterol efflux: ABCA1 and ABCG1. In wild-type mice, ABCA1 was localized in the apical part of the apical cells in segments 1 and 2 at 4 (**Fig. 4A**, a–e) and 9 months (Fig. 4A, c–g). In LXR$^{-/-}$ mice both at 4 and 9 months of age, a complete loss of the
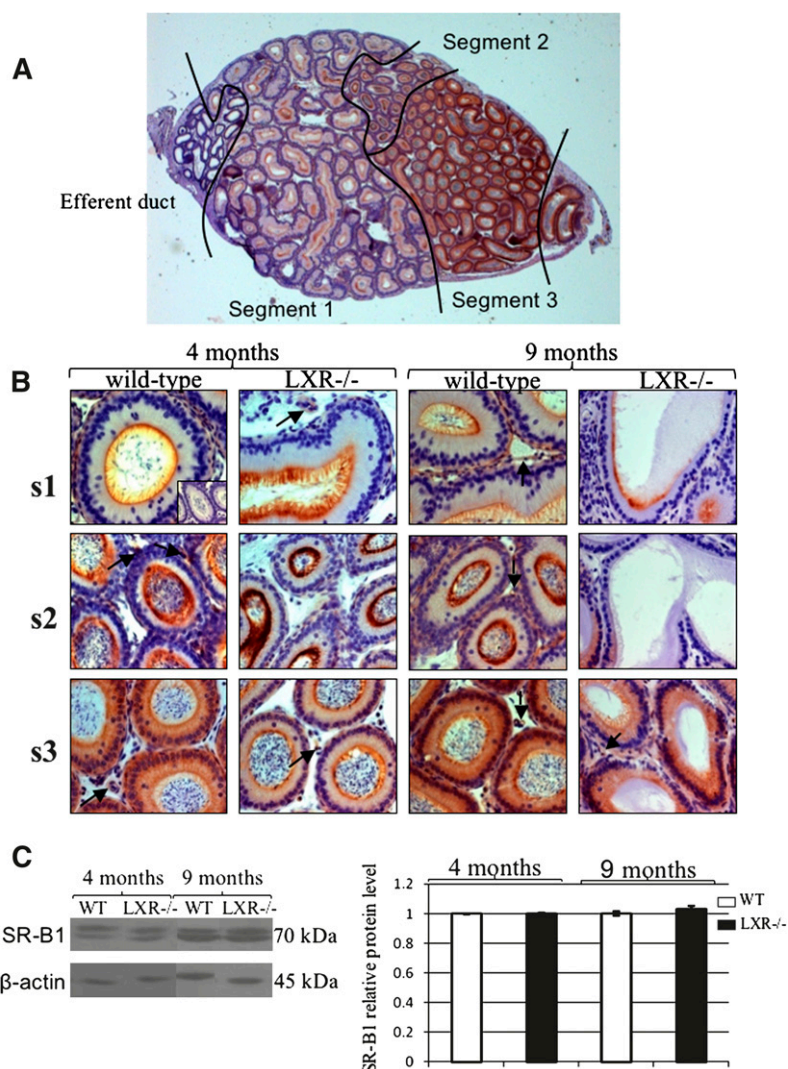
Fig. 3. SR-B1 expression and localization do not change with the genotype or the age. A: SR-B1 immunoperoxydase staining in caput epididymidis from wild-type mice. Magnification ×25. B: SR-B1 immunoperoxydase staining in segment1 (s1), segment 2 (s2), and segment 3 (s3) caput epididymidis from wild-type and LXR$^{-/-}$ mice at 4 and 9 months of age. Each photomicrograph is representative of three different experiments made on three different individuals. Inset shows negative control. Original magnification ×630. C: Relative level of SR-B1 protein in caput and cauda epididymidis from wild-type and LXR$^{-/-}$ mice at 4 and 9 months of age. Histograms are expressed as mean ± SEM of three different experiments made on three different animals using β-actin as an internal standard for quantification.
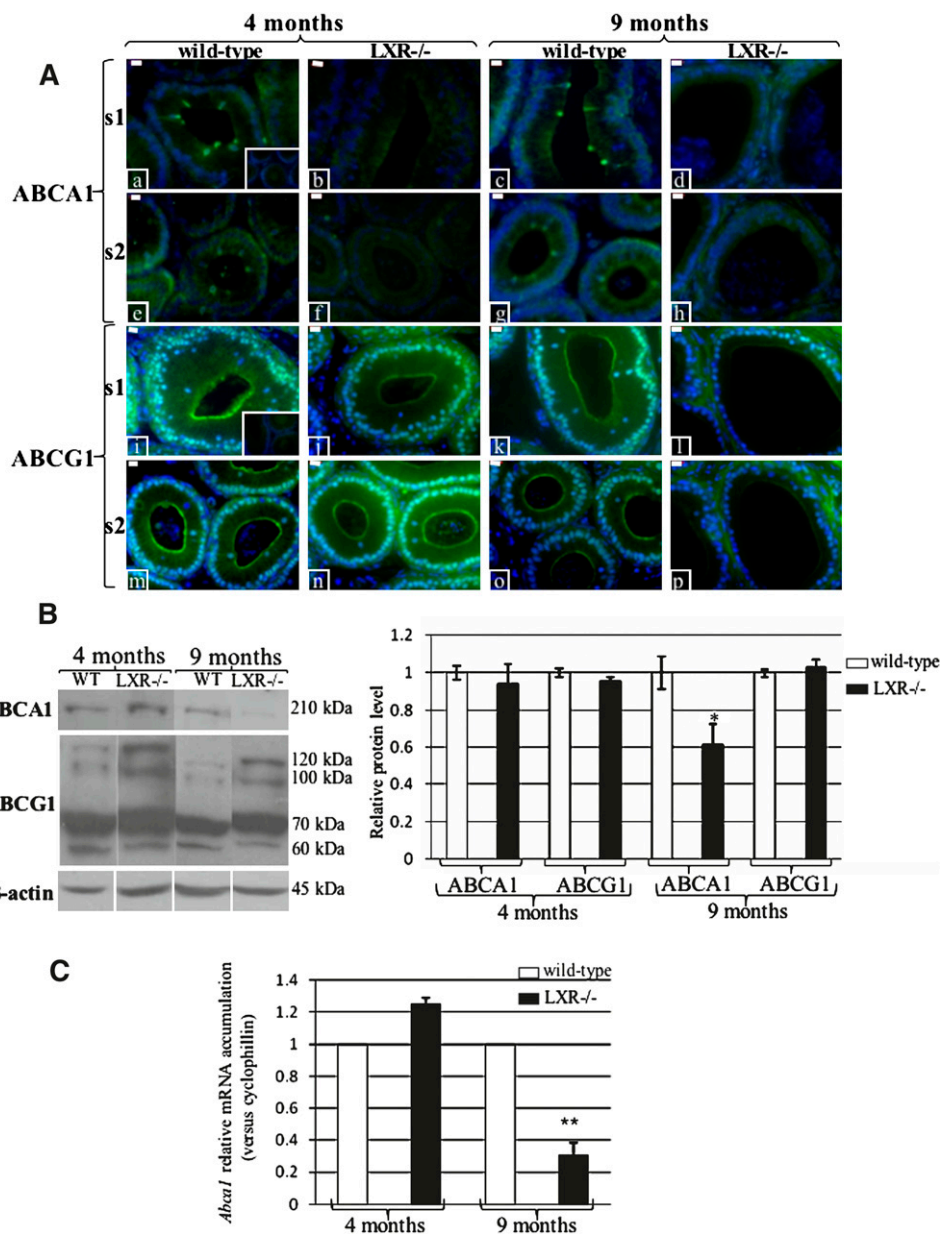
Fig. 4. ABCA1 loss may be responsible for neutral lipid accumulations observed in LXR$^{-/-}$ mice. A: ABCA1 (a–h) and ABCG1 (i–p) immunofluorescence staining in segment 1 (s1) and segment 2 (s2) caput epididymidis from wild-type and LXR$^{-/-}$ mice at 4 and 9 months of age. Bars = 10 μm. Each photomicrograph is representative of three different experiments made on three different individuals. Inset shows negative control. B: Relative proteins levels of ABCA1 and ABCG1 in caput epididymidis at 4 and 9 months from wild-type and LXR$^{-/-}$ mice. Histograms are expressed as mean ± SEM of three different experiments using β-actin for relative quantification made on three different animals. C: Relative level of *abca1* mRNAs in caput epididymides at 4 and 9 months. Histograms are expressed as a normalized value of the expression level in lxr$^{-/-}$ animals versus an arbitrary value of 1 in the wild-type animals. Each value is the mean ± SEM of three measurements performed on three different animals using cyclophillin as internal standard. *$P < 0.05$ and **$P < 0.01$ compared with wild-type mice.

ABCA1 staining was observed (Fig. 4A, b–d and f–h). ABCG1 presented staining both in the nucleus of epithelial cells and on the apical membrane of the epithelium, in segments 1 and 2 irrespective of cell type and genotype (Fig. 4A, i–p). Accumulation of ABCA1 and ABCG1 was determined by Western blot in protein extracts made with entire caput epididymides (Fig. 4B). Contrary to the histochemical data presented in Fig. 4A, no difference was found for ABCA1 at 4 months of age in the wild-type and LXR$^{-/-}$ mice, whereas a significant 1.6-fold decrease was found in the LXR$^{-/-}$ mice compared with wild-type mice ($P < 0.05$) at 9 months of age. This apparent discrepancy (Fig. 4A versus Fig. 4B) reflects that ABCA1 protein levels in the caput epididymides of LXR$^{-/-}$ animals at 4 months of age are modified in a discrete manner (i.e, solely in apical cells of segments 1 and 2) that is not sufficient at that
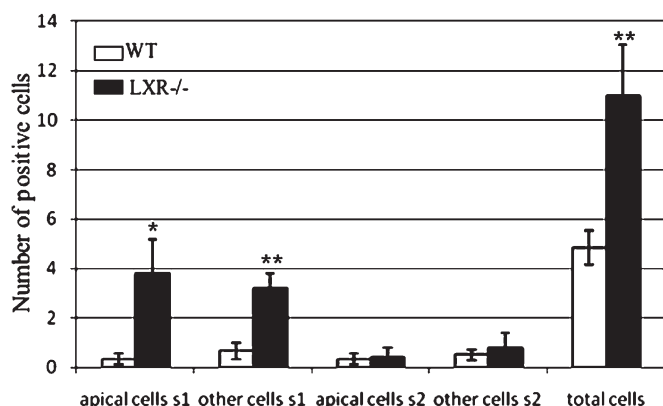
age to modify the overall quantity of ABCA1 protein in the entire caput. For ABCG1, no significant differences in accumulation of the four variants, the 60, 70, 100, and 120 kDa protein bands, was found at 4 and 9 months of age in wild-type and LXR$^{-/-}$ mice. However, there was a clear change in the relative representation of three of four variants since we recorded a decrease of the 60 kDa ABCG1 variant and an increase of the 100 and 120 kDa ABCG1 variants. Western blot data were correlated with quantitative RT-PCR analysis (Fig. 4C) showing that *abca1* mRNA accumulation did not change in the caput epididymides of 4-month-old LXR$^{-/-}$ animals, while a 70% decrease was recorded in the caput epididymides of 9-month-old animals when compared with controls ($P < 0.001$). These data lead us to suggest that ABCA1 is involved in neutral lipid accumulations.

CE accumulation enhances apoptosis in segment 1 epithelial cells

Since neutral lipid accumulations are known to cause apoptosis in some cell types (18), we carried out TUNEL staining experiments on caput epididymidis from wild-type and LXR$^{-/-}$ mice at 4 months. The number of apoptotic cells was significantly increased (2.3-fold) in the caput epididymidis of LXR$^{-/-}$ mice compared with controls (**Fig. 5**; $P < 0.01$) but only in segment 1 and was not restricted to a particular cell type. However, apoptosis was greater in apical cells (11.4-fold increase compared with the wild-type) compared with the other epithelial cell type (4.8-fold increase compared with the wild-type), suggesting a correlation between CE accumulations and apoptosis in apical cells.

abca1 is regulated by LXR in the caput epididymidis

To determine whether *abca1* was physiologically regulated by LXR in the caput epididymidis, 8-month-old wild-type mice were given a Western diet for 7 weeks. This diet has already been shown to activate LXR (19). Data presented in **Fig. 6** demonstrate that ABCA1 accumulation was clearly increased in the caput epididymides of wild-type mice fed the Western diet (Fig. 6; $P < 0.05$). The epididymal epithelium thus responds to the cholesterol enriched diet by enhancing ABCA1 protein via LXR stimulation.

The absence of LXR leads to modifications in neutral lipids FA composition

In previous research, we showed that *srebp1c* was decreased in caput epididymidis of LXR$^{-/-}$ mice (15), suggesting possible modifications in the fatty acid content. PL fatty acids and neutral lipid fatty acids of caput epididymides were extracted and analyzed (**Fig. 7A**, B). No significant changes occurred in the PL fatty acid profile, except for the C22:4n-6 (docosatetraenoic acid; $P < 0.05$). Decreased C16:0 (palmitic acid) and C18:1n-9 *cis* (oleic acid; $P < 0.05$) and increased C16:1n-7 (palmitoleic acid; $P < 0.05$), C20:4n-6 (arachidonic acid; $P < 0.01$), and C22:4n-6 ($P < 0.05$) were observed in neutral lipid fatty acid contents in LXR$^{-/-}$ compared with wild-type mice.

DISCUSSION

This study investigated the role of LXR nuclear receptors in the regulation of cholesterol homeostasis in caput epididymidis, using a comparison between wild-type and LXR$^{-/-}$ male mice. Nile Red staining allowed us to show that CEs were mainly accumulated in the apical cells of caput epididymidis segments 1 and 2 leading to increased cell apoptosis. This accumulation of CEs was linked to the loss of ABCA1 expression in segments 1 and 2. ABCA1 has already been described to be important for male fertility (20). Our data also showed precisely the ABCA1 distribution in the proximal epididymis. In caput segments 1 and 2, ABCA1 was expressed in the apical cells, while in the more distal caput (segment 3 and downwards) ABCA1 staining was found in principal cells. Recently, Morales et al. (21) also reported the detection of ABCA1 in the principal cells of an undefined mouse caput segment, most likely a segment posterior of segment 2. Interestingly, ABCA1 accumulation was only lost in the segments 1 and 2 of LXR$^{-/-}$ animals, while posterior of segment 2, ABCA1 distribution was unchanged, suggesting a specific regulation of *abca1* by LXR along the epididymis. Confirming this pattern of regulation, segments 1 and 2 were the sole segments showing disturbed epithelia in LXR$^{-/-}$ mice (12). The fact that CE accumulations were mainly due to a defect in ABCA1 representation was confirmed by quantitative RT-PCR analysis of mRNAs involved either in de novo cholesterol synthesis or cholesterol esterification. Expression levels of *srebp-2*, *hmg-CoA-red*, *hmg-coA-synt*, *acat1*, and *acat2* were measured, and a significant difference (decrease) was only observed for *srebp-2* and *hmg-coA-synt*. These results suggest that neither endogenous cholesterol synthesis nor esterification was modified in LXR$^{-/-}$ mice. The decrease recorded in *srebp-2* and *hmg-coA-synt* expression could be a consequence of CE accumulations

Fig. 5. Apoptosis is more important in caput epididymidis of LXR$^{-/-}$ mice. DNA breaks immunofluorescence staining by the TUNEL method. Positive cells were counted in segment 1 (s1), segment 2 (s2), and whole caput epididymidis. Histograms are expressed as mean ± SEM of counted cells per segment in three different experiments with three different individuals. *$P < 0.05$ and **$P < 0.01$ compared with wild-type mice.
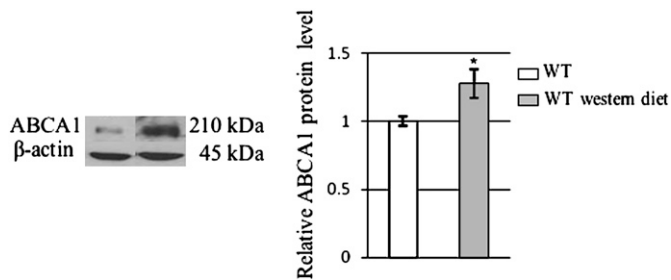
Fig. 6. ABCA1, a target gene of LXR, is overexpressed in caput epididymidis under a cholesterol-enriched diet. Relative proteins levels of ABCA1 in caput epididymidis in 8-month-old wild-type mice fed during 7 weeks with a Western diet (1.25% cholesterol). Histograms are expressed as mean ± SEM of three different experiments using β-actin for relative quantification made on three different animals. *$P < 0.05$ compared with wild-type mice

as previously demonstrated in hamster (22). In parallel, apoE expression, an apoprotein acceptor of effluxed cholesterol, was also investigated and no change at all was recorded (data not shown).

At 4 months of age, only ABCA1 staining in apical cells of segments 1 and 2 in LXR$^{-/-}$ mice was lost. Since mRNA extractions were carried out on the whole caput, it is likely that the variations seen in *abca1* expression were not detectable. However, only ABCA1 protein level was altered, whereas for ABCG1, we have observed only discrete changes in the representation of its splicing variants [(23); see above]. To our knowledge, neither different cellular distribution nor specific roles have yet been ascribed to these distinct *abcg1* variants.

To determine cholesterol fluxes in caput epididymidis more precisely, we investigated the cellular location of lipoprotein receptors SR-B1 and LDL-R. As no evidence of LDL-R was shown, it appeared that the main receptor represented in the caput epithelium was SR-B1, which mediates selective uptake of CEs from HDL to cells (24), thus being a possible candidate in the CE accumulations observed in LXR$^{-/-}$ male mice. However, our results overruled this hypothesis, since no difference in SR-B1

accumulation was found between wild-type and LXR$^{-/-}$ mice. In addition, our data also showed specific SR-B1 localization in the various epididymal segments.

The LXR$^{-/-}$ mice also present abnormalities in their epididymal fatty acid metabolism. We showed earlier that the expression level of *srebp-1c* in the caput epididymidis was downregulated in these mice and that little differences were seen in the fatty acid content of both the PL and neutral lipid fractions (15). More refined fatty acid evaluations realized here on caput epididymides of LXR$^{-/-}$ animals show an increase in the relative proportions of palmitoleic acid (C16:1 n-7) in the neutral lipid fraction, correlated with a decrease of palmitic acid (C16:0). These changes are in accordance with intracellular CE accumulations, as the principal fatty acid esterifying the cholesterol moieties is palmitoleic acid.

The association of CE accumulations and apoptosis that we revealed by TUNEL assays in the apical cells of segment 1 has already been reported elsewhere (18). Apoptosis of apical cells could be the starting point of epididymal epithelium destructuration. This point raises the question of the physiological role of this particular cell type in the proximal region of the epididymal duct. Apical cells are
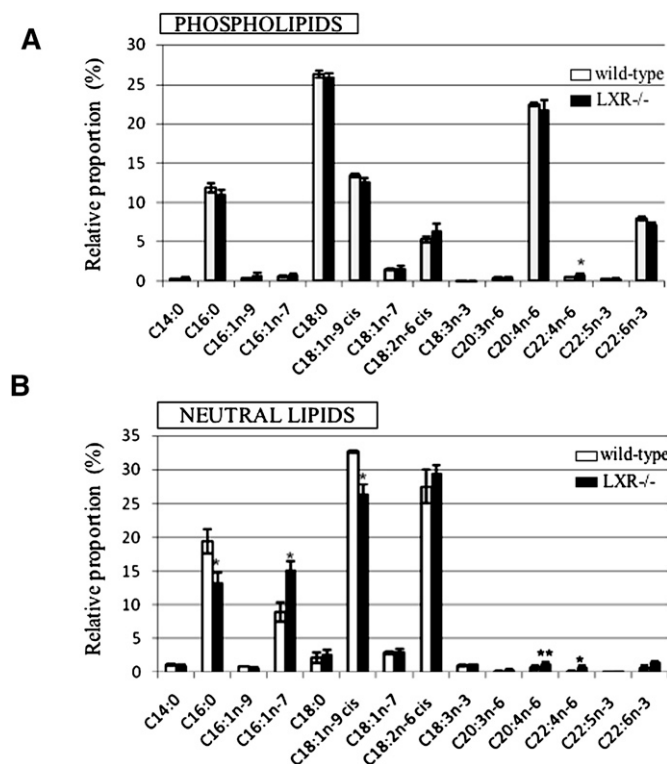
Fig. 7. PLs and neutral lipids fatty acids profiles of 4-month-old wild-type and LXR$^{-/-}$ mice. Measurement of PL fatty acids (A) and neutral lipid (B) fatty acids of caput epididymidis in wild-type and LXR$^{-/-}$ mice at 4 months of age. Histograms are expressed as mean ± SEM of three different measurements made on three pools of tissues, each made of three different animals. *$P < 0.05$ and **$P < 0.01$ compared with wild-type mice.

Cholesterol homeostasis in the proximal mouse epididymis 1773

known to be rich in mitochondria and to show endocytic activity (25). It was suggested that they are involved in fluid acidification because of their high carbonic anhydrase content (26) as well as in sodium transport and chloride fluxes (27). Our data suggest that these cells are also critical for cholesterol trafficking in the proximal epididymis.

Based on our data, we propose a model of cholesterol fluxes in this organ. In segment 1, lipoproteins could reach the epithelium through fenestrated blood capillaries and be processed by SR-B1. Cholesterol could then be transferred to the lumen via ABCA1 in the apical cells and ABCG1 in the principal cells. This would imply cooperation between these two cell types, as ABCA1 transfers cholesterol and PLs to lipid-poor apoproteins, such as apoA1, apoE, and apoJ, whereas ABCG1 effluxes cholesterol to mature HDL but not to lipid-poor apoproteins [as reviewed in (28)]. Such cooperation in these two ABC transporters has already been shown in vitro (28). This hypothesis is supported by the fact that apoE has already been shown to be expressed in the caput epididymidis [this study and (29)]. SR-B1 apical staining in the caput segment 1 suggests that exchanges might occur between the epithelium and testicular fluid entering the organ. The stronger staining for SR-B1 obtained on the microvilli of segment 2 caput epithelial cells suggests an intense cholesterol reabsorption process in that particular segment. Downstream, the subsequent intracytoplasmic cellular localization of SR-B1 (segment 3) is here in favor of intracellular trafficking of cholesterol and interaction of late endosomes with lysosomes (30). Intercellular exchanges in the epithelium might also occur since SR-B1 was also detected on the lateral membranes (from caput segment 4 to cauda; data not shown). Such intercellular exchanges have been shown elsewhere (31).

In conclusion, this study showed for the first time that regulation of cholesterol homeostasis in mice caput epididymidis is a cell and segment-specific process regulated in part by LXR. Our data offer new perspectives for study of the molecular mechanisms related to cholesterol maturation of sperm cells and emphasize the already important role devoted to the proximal caput epididymidis in the posttesticular sperm cell maturation process. It has demonstrated a new role played by the so-called apical cells of the proximal caput epithelium in cholesterol homeostasis and epididymis physiology.

REFERENCES

1. Turner, T. T. 1995. On the epididymis and its role in the development of the fertile ejaculate. *J. Androl.* **16:** 292–298.

2. Jones, R. C. 1999. To store or mature spermatozoa? The primary role of the epididymis. *Int. J. Androl.* **22:** 57–67.

3. Hinton, B. T., M. A. Palladino, D. Rudolph, Z. J. Lan, and J. C. Labus. 1996. The role of the epididymis in the protection of spermatozoa. *Curr. Top. Dev. Biol.* **33:** 61–102.

4. Jones, R. 1998. Plasma membrane structure and remodelling during sperm maturation in the epididymis. *J. Reprod. Fertil. Suppl.* **53:** 73–84.

5. Rejraji, H., B. Sion, G. Prensier, M. Carreras, C. Motta, J. M. Frenoux, E. Vericel, G. Grizard, P. Vernet, and J. R. Drevet. 2006. Lipid remodeling of murine epididymosomes and spermatozoa during epididymal maturation. *Biol. Reprod.* **74:** 1104–1113.

6. Christova, Y., P. S. James, T. G. Cooper, and R. Jones. 2002. Lipid diffusion in the plasma membrane of mouse spermatozoa: changes during epididymal maturation, effects of pH, osmotic pressure, and knockout of the c-ros gene. *J. Androl.* **23:** 384–392.

7. Cooper, T. G., G. M. Waites, and E. Nieschlag. 1986. The epididymis and male fertility. A symposium report. *Int. J. Androl.* **9:** 81–90.

8. Bedford, J. M. 1983. Significance of the need for sperm capacitation before fertilization in eutherian mammals. *Biol. Reprod.* **28:** 108–120.

9. Han, Y., C. J. Haines, and H. L. Feng. 2007. Role(s) of the serine/ threonine protein phosphatase 1 on mammalian sperm motility. *Arch. Androl.* **53:** 169–177.

10. Peet, D. J., B. A. Janowski, and D. J. Mangelsdorf. 1998. The LXR: a new class of oxysterol receptors. *Curr. Opin. Genet. Dev.* **8:** 571–575.

11. Volle, D. H., and J. M. Lobaccaro. 2007. Role of the nuclear receptors for oxysterols LXR in steroidogenic tissues: beyond the "foie gras", the steroids and sex? *Mol. Cell. Endocrinol.* **265–266:** 183–189.

12. Frenoux, J. M., P. Vernet, D. H. Volle, A. Britan, F. Saez, A. Kocer, J. Henry-Berger, D. J. Mangelsdorf, J. M. Lobaccaro, and J. R. Drevet. 2004. Nuclear oxysterol receptors, LXR, are involved in the maintenance of mouse caput epididymidis structure and functions. *J. Mol. Endocrinol.* **33:** 361–375.

13. Volle, D. H., K. Mouzat, R. Duggavathi, B. Siddeek, P. Dechelotte, B. Sion, G. Veyssiere, M. Benahmed, and J. M. Lobaccaro. 2007. Multiple roles of the nuclear receptors for oxysterols liver X receptor to maintain male fertility. *Mol. Endocrinol.* **21:** 1014–1027.

14. Robertson, K. M., G. U. Schuster, K. R. Steffensen, O. Hovatta, S. Meaney, K. Hultenby, L. C. Johansson, K. Svechnikov, O. Söder, and J-A. Gustafsson. 2005. The liver X receptor β is essential for maintaining cholesterol homeostasis in the testis. *Endocrinology.* **146:** 2519–2530.

15. Saez, F., E. Chabory, R. Cadet, P. Vernet, S. Baron, J. M. Lobaccaro, and J. R. Drevet. 2007. Liver X receptors and epididymal epithelium physiology. *Asian J. Androl.* **9:** 574–582.

16. Lee, P. D., S. E. Noble-Topham, R. S. Bell, and I. L. Andrulis. 1996. Quantitative analysis of multidrug resistance gene expression in human osteosarcomas. *Br. J. Cancer.* **74:** 1046–1050.

17. Juaneda, P., and G. Roquelin. 1985. Rapid and convenient separation of phospholipids and non phosphorus lipids from rat heart using silica cartridges. *Lipids.* **20:** 40–41.

18. Nakamura, K., M. A. Kennedy, A. Baldan, D. D. Bojanic, K. Lyons, and P. A. Edwards. 2004. Expression and regulation of multiple murine ATP-binding cassette transporter G1 mRNAs/isoforms that stimulate cellular cholesterol efflux to high density lipoprotein. *J. Biol. Chem.* **279:** 45980–45989.

19. Veri, J. P., L. Hermo, and B. Robaire. 1993. Immunocytochemical localization of the Yf subunit of glutathione S-transferase P shows regional variation in the staining of epithelial cells of the testis, efferent ducts, and epididymis of the male rat. *J. Androl.* **14:** 23–44.

20. Healy, D. A., R. W. Watson, and P. Newsholme. 2003. Polyunsaturated and monounsaturated fatty acids increase neutral lipid accumulation, caspase activation and apoptosis in a neutrophil-like, differentiated HL-60 cell line. *Clin. Sci. (Lond.).* **104:** 171–179.

21. Morales, C. R., A. L. Marat, X. Ni, Y. Yu, R. Oko, B. T. Smith, and W. S. Argraves. 2008. ATP-binding cassette transporters ABCA1, ABCA7, and ABCG1 in mouse spermatozoa. *Biochem. Biophys. Res. Commun.* **376:** 472–477.

22. Iddon, C. R., J. Wilkinson, A. J. Bennett, J. Bennett, A. M. Salter, and J. A. Higgins. 2001. A role for smooth endoplasmic reticulum membrane cholesterol ester in determining the intracellular location and regulation of sterol-regulatory-element-binding protein-2. *Biochem. J.* **358:** 415–422.

23. Nakamura, M. T., Y. Cheon, Y. Li, and T. Y. Nara. 2004. Mechanisms of regulation of gene expression by fatty acids. *Lipids.* **39:** 1077–1083.

24. Acton, S., A. Rigotti, K. T. Landschulz, S. Xu, H. H. Hobbs, and M. Krieger. 1996. Identification of scavenger receptor SR-BI as a high density lipoprotein receptor. *Science.* **271:** 518–520.

25. Moore, H. D., and J. M. Bedford. 1979. The differential absorptive activity of epithelial cells of the rat epididymus before and after castration. *Anat. Rec.* **193:** 313–327.

26. Rosen, S., J. A. Oliver, and P. R. Steinmetz. 1974. Urinary acidification and carbonic anhydrase distribution in bladders of Dominican and Colombian toads. *J. Membr. Biol.* **15:** 193–205.

27. Voute, C. L., and W. Meier. 1978. The mitochondria-rich cell of frog skin as hormone-sensitive "shunt-path". *J. Membr. Biol.* **40:** 151–165.

28. Oram, J. F., and A. M. Vaughan. 2006. ATP-Binding cassette cholesterol transporters and cardiovascular disease. *Circ. Res.* **99:** 1031–1043.

29. Olson, L. M., X. Zhou, and J. R. Schreiber. 1994. Immunolocalization of apolipoprotein E in testis and epididymis of the rat. *Biol. Reprod.* **50:** 535–542.

30. Ahras, M., T. Naing, and R. McPherson. 2008. Scavenger receptor class B type I localizes to a late endosomal compartment. *J. Lipid Res.* **49:** 1569–1576.

31. Akpovi, C. D., S. R. Yoon, M. L. Vitale, and R-M. Pelletier. 2006. The predominance of one of the SR-B1 isoforms is associated with increased esterified cholesterol levels not apoptosis in mink testis. *J. Lipid Res.* **47:** 2233–2247.